Wessely, Johannes ; Chytrý, Kryštof ; Gattringer, Andreas ; Hausharter, Johannes ; Helm, Norbert ; Hülber, Karl ; Moser, Dietmar ; Abdaladze, Otar ; Andrews, Christopher ; Barni, Elena ; Barolin, Debora ; Benito-Alonso, José-Luis ; von Büren, Raphael S. ; Carbognani, Michele ; Carnicero, Pau ; Di Cecco, Valter ; Choler, Philippe ; Dick, Jan ; Fernández-Calzado, Rosa ; De Frenne, Pieter ; Lino, Mary Carolina García ; Ghosn, Dany ; Gigauri, Khatuna ; Graae, Bente J.; Hilpold, Andreas ; Jiménez, Juan J. ; Kagerl, Katharina ; Kanka, Róbert ; Kollár, Jozef ; Lamprecht, Andrea ; Lembrechts, Jonas ; Lenoir, Jonathan ; Lorite, Juan ; Nyktas, Panagiotis ; Pușcaș, Mihai ; Randin, Christophe F.; Rixen, Christian ; Rossi, Graziano ; Saccone, Patrick ; Ursu, Tudor Mihai; Vanneste, Thomas ; Varricchione, Marco ; Vittoz, Pascal ; Winkler, Manuela ; Wipf, Sonja ; Pauli, Harald ; Dullinger, Stefan. 2026. **Rising plant extinction rates on European mountain summits**.

The definitive version was published in *Science*, 393 (6815). 1021-1026. https://doi.org/10.1126/science.aed2974

Title:
Rising plant extinction rates on European mountain summits

Authors:
Johannes Wessely[1]*, Kryštof Chytrý[1], Andreas Gattringer[1, †], Johannes Hausharter[1,2], Norbert Helm[1,2], Karl Hülber[1], Dietmar Moser[1], Otar Abdaladze[3], Christopher Andrews[4], Elena Barni[5], Debora Barolin[6], José-Luis Benito-Alonso [7, 8], Raphael S. von Büren[9, 10], Michele Carbognani[11], Pau Carnicero[12, 13], Valter Di Cecco[14], Philippe Choler[15], Jan Dick[4], Rosa Fernández-Calzado[16], Pieter De Frenne[17], Mary Carolina García Lino[18, 19], Dany Ghosn[20], Khatuna Gigauri[21], Bente J. Graae[22], Andreas Hilpold[23], Juan J. Jiménez [7], Katharina Kagerl[18, 19], Róbert Kanka[24], Jozef Kollár[24], Andrea Lamprecht[18, 19], Jonas Lembrechts[25, 26], Jonathan Lenoir[27], Juan Lorite[16, 28], Panagiotis Nyktas[29, 30], Mihai Pușcaș[31, 32], Christophe F. Randin[33, 34, 35], Christian Rixen[36, 37], Graziano Rossi[38], Patrick Saccone[18, 19, 39], Tudor Mihai Ursu[40], Thomas Vanneste[17], Marco Varricchione[41], Pascal Vittoz[33], Manuela Winkler[18, 19], Sonja Wipf[9, 10, 36], Harald Pauli[18, 19] & Stefan Dullinger[1]

Affiliations:
[1]Department of Botany and Biodiversity Research, University of Vienna; 1030 Vienna, Austria.

[2]Vienna Doctoral School of Ecology and Evolution (VDSEE), University of Vienna; 1030 Vienna, Austria.

[3]School of Natural Sciences and Medicine, director of Alpine Ecosystems Research Program, Institute of Ecology, Ilia State University; 5 of Cholokashvili Ave. 0179, Tbilisi, Georgia.

[4]UK Centre for Ecology & Hydrology (UKCEH); Bush Estate, Penicuik, EH26 0QB, UK.

[5]Department of Life Sciences and Systems Biology, University of Turin; Turin, Italy.

[6]Ente di Gestione delle Aree Protette delle Alpi Cozie, Salbertrand; Turin, Italy.

[7]Instituto Pirenaico de Ecología, Consejo Superior de Investigaciones Científicas; Jaca, Spain.

[8]GLORIA-ARAGÓN coordination, Jolube Botanical Consultant; Jaca, Spain.

[9]Department of Research and Monitoring, Swiss National Park; Zernez, Switzerland.

[10]Department of Environmental Sciences, University of Basel; Basel, Switzerland.

[11]Department of Chemistry, Life Sciences and Environmental Sustainability, University of Parma; Parco Area delle Scienze 11/A, 43124 Parma, Italy.

[12]Department of Botany, University of Innsbruck; Innsbruck, Austria.

[13]Department of Animal Biology, Plant Biology and Ecology, Autonomous University of Barcelona; Bellaterra, Spain.

[14]Maiella Seed Bank, Maiella National Park, loc. Colle Madonna; Lama dei Peligni, 66010, Italy.

[15]Univ. Grenoble Alpes, Univ. Savoie Mont Blanc, CNRS, LECA, F-38000 Grenoble, France

[16]Department of Botany, University of Granada; 18071 Granada, Spain.

[17]Forest & Nature Lab, Ghent University; Geraardsbergsesteenweg 267, 9090 Gontrode, Belgium.

[18]GLORIA co-ordination, Institute for Interdisciplinary Mountain Research, Austrian Academy of Sciences; 1180 Vienna, Austria.

[19]GLORIA co-ordination, Institute of Botany, Department of Ecosystem Management, Climate and Biodiversity, BOKU University; 1180 Vienna, Austria.

[20]Department of Geoinformation in Environmental Management - Alsyllio Agrokepiou, CIHEAM-Mediterranean Agronomic Institute of Chania; 73100 Chania, Greece.

[21]School of Environmental Management and Policy, Georgian Institute of Public Affairs; 0108 Tbilisi, Georgia.

[22]Department of Biology, Norwegian University of Science and Technology (NTNU); 7491 Trondheim, Norway.

[23]Institute for Alpine Environment, Eurac Research; Bolzano/Bozen, Italy.

[24]Institute of Landscape Ecology Slovak Academy of Sciences; Štefánikova 3, 814 99, Bratislava, Slovakia.

[25]Ecology & Biodiversity, Utrecht University; Utrecht, the Netherlands.

[26]Plants & Ecosystems (PLECO), University of Antwerp; Antwerp, Belgium.

[27]UMR CNRS 7058 “Ecologie et Dynamique des Systèmes Anthropisés” (EDYSAN), Université de Picardie Jules Verne; 1 rue des Louvels, 80000 Amiens, France.

[28]Interuniversity Institute for Earth System Research, University of Granada; 18006 Granada, Spain.

[29]Faculty of Geo-information Science and Earth Observation (ITC), University of Twente; PO Box 217, Enschede, 7500 AE, Netherlands.

[30]Natural History Museum of Crete, School of Sciences and Engineering, University of Crete, 71409 Heraklion, Greece

[31]Department of Taxonomy and Ecology, Babeş- Bolyai University; Cluj- Napoca, Romania.

[32]Alexandru Borza Botanic Garden, Babeş- Bolyai University; Cluj- Napoca, Romania.

[33]Faculty of Geosciences and Environment, Institute of Earth Surface Dynamics, University of Lausanne; 1015 Lausanne, Switzerland.

[34]Interdisciplinary Centre for Mountain Research, University of Lausanne; Lausanne, Switzerland.

[35]Fondation Aubert, Jardin Flore-Alpe et Centre Alpien de Phytogeographie CAP; Champex-Lac, Switzerland.

[36]WSL-Institute for Snow and Avalanche Research SLF; Davos, Switzerland.

[37]Climate Change, Extremes and Natural Hazards in Alpine Regions Research Centre CERC; Davos Dorf, Switzerland.

[38]Department of Earth and Environmental Sciences, University of Pavia; Via Sant Epifanio 14, 27100, Pavia, Italy.

[39]Institute of Botany of the Czech Academy of Sciences; Zámek 1, Průhonice, CZ-252 43, Czech Republic.

[40]Institute of Biological Research Cluj-Napoca - subsidiary of NIRDBS Bucharest; 400015 Cluj-Napoca, Romania.

[41]Department of Biosciences and Territory, University of Molise; 86090 Pesche, Italy.

*Corresponding author: johannes.wessely@univie.ac.at

†Present address: Faculty of Physics, Aerosol Physics and Environmental Physics, University of Vienna; Vienna, Austria

Abstract:

Climate change increases plant species richness in alpine ecosystems. However, to what extent this diversity enrichment masks extinction dynamics of resident species remains elusive. Here, we use floristic resurvey data from 896 permanent vegetation plots across 62 European mountain summits to show that local extinctions have increased over the past 21 years. Extinction rates rose with the magnitude of warming, and species were more likely to go extinct towards their low-elevation range margins and in communities undergoing stronger thermophilization. Moreover, local extinctions were significantly related to preceding abundance declines, which can hence serve as an early warning signal. These findings suggest that despite increasing plant species richness, plant assemblages above the treeline face an accelerating, but so far neglected loss of their most characteristic species.

Main Text:

Vascular plant species richness on mountain summits has increased during recent decades (*1, 2*). The likely driver of this species accumulation is the accelerating rate of climate warming at higher elevation (*3*), which has made previously inhospitable sites more amenable to vascular plant life and enabled less cold-tolerant species from lower-elevation habitats to shift or expand upslope and colonize mountain summits (*2, 4-6*). However, this increase in species richness dominated by lower-elevation species may obscure a loss of resident specialists (*7*). Identifying and quantifying this possible loss is important as high-elevation floras tend to be rich in geographically restricted and often functionally unique or distinct species (*8, 9*). Extinctions from this unique species pool can thus have disproportionate effects on functional and phylogenetic diversity, endemism and rarity (*10, 11*).

Local and regional studies suggest that species above the treeline do indeed sort into 'winners' and 'losers' in terms of abundance change with climate warming, and that specialists of highest elevations are disproportionately frequent among the 'losers' (*12-14*). However, no continental-scale analysis has so far provided a systematic assessment of the magnitude of recent species losses in high-mountain plant communities or potential patterns of vulnerability among species and populations. Moreover, local and regional-scale findings have often been based on a single resurvey of historical observations, where directed abundance trends can most easily be confounded with stochastic population fluctuation or observation error (*15, 16*). Whether the documented abundance declines are early-warning signs of pending local- or larger-scale extinctions remains hence to be evaluated.

The Global Observation Research Initiative in Alpine Environments (GLORIA, *17*) is the largest systematic monitoring scheme of climate effects on mountain summit floras (*18*). In Europe, its core sampling network consists of 62 summits distributed across 16 mountain regions (Fig. 1) that were surveyed four times, in 7-year intervals, between 2001 and 2022 (with a few minor deviations, see 19 for details). During each survey, on each summit, the full list of vascular plants, together with their abundance (ground cover, visual estimation) were recorded on 16 permanent 1 m × 1 m plots. Based on these data, we here analysed temporal trends in local extinctions and their relationship with the magnitude of climate warming. We refer to local extinction as the disappearance of a species recorded in one, but not re-recorded in the consecutive survey, although we do not know whether the species persisted on the same summit or in the same region outside of the surveyed plots. For the species that were present in the first survey, we moreover evaluated whether the likelihood of local extinction events was related to a preceding decrease of their cover and the position of the plot within the species' elevational range, and whether extinctions were more likely in communities undergoing a more pronounced change towards predominance of warmth-demanding species, so-called thermophilization (*20*). To account for slight variation in observation methods between surveys, we used a resampling approach in the analyses and report results as means and standard deviations of resamples (see 19 for details). Temporal and geographical trends in local extinctions were assessed on the level of sampled plots, as well as on the aggregated levels of summits and mountain regions.

Rates and temporal trends of local extinctions, and their relationship to climatic trends

Local extinction events were observed frequently in each re-survey. Across the three re-surveys, the number of such extinction events varied as follows: 980 to 1451 ± 9 at the plot level, 118 to 185 ± 4 at the summit level, and 57 to 99 ± 2 at the mountain region level. These numbers correspond to 11.1% to 15.7% ± 0.1%, 6.7% to 9.9% ± 0.2%, and 5.5% to 8.9% ± 0.2% of all species observations at the plot, summit, and mountain region level, respectively

(see table S1). However, a considerable percentage (34.2% ± 0.2%) of the plot-level extinctions documented in the second or third survey were followed by re-observation of the focal species during one of the subsequent surveys, either due to real extinction and colonization dynamics, lack of above-ground appearance of species in a certain year, or due to intermittent observer errors. In the most conservative accounting, which only considers species present in the first, but in none of the three consecutive surveys, there were 578, 62, and 31 extinction events, corresponding to 6.5%, 3.5%, and 3% of the species observations on the plot, summit, and mountain region level, respectively.

Using generalized linear mixed-effects models for proportion data (see 19 for details), we found that local extinction rates significantly increased over time, i.e., with each consecutive re-survey, on each level of aggregation, i.e., on the plot, summit and mountain region level (Fig. 2, Fig. 3A and table S2). Extinction rates rose in parallel with the total vascular plant cover per plot and species richness per plot and summit (Fig 3B, table S3 and S4). However, when fitting these extinction-rate models we included local extinctions of all species, even if they were re-observed in consecutive surveys. This was necessary because the chance for an apparently extinct species to re-appear decreases with the number of subsequent surveys. Omitting local extinctions followed by re-observations would hence result in rising extinction rates *per se.* To assess whether the detected temporal trend is attributable to increased rates of natural fluctuation and observer error or rather indicates a rise of local extinction rates we thus fitted two additional mixed-effects models for proportion data (see *19*). In these additional models, we separately tested whether the likelihood of a transition of type presence-absence-presence and of type presence-absence-absence has increased between the earlier (2001-2008-2015) and later (2008-2015-2022) three surveys. We thereby interpreted the latter type of transition as an indication of real local extinction events. We found that on all three levels of aggregation only transitions of type presence-absence-absence became more frequent (estimate = 0.26 ± 0.009, $p < 0.001$, estimate = 0.37 ± 0.03, $p = 0.016 \pm 0.010$ and estimate = 0.45 ± 0.030, $p = 0.04 \pm 0.015$, respectively). These results suggest that natural fluctuation and observer error have not increased over time, but that the increase in extinctions drives the observed trend.

To evaluate whether climate warming could be the driver behind rising local extinction rates, we quantified the magnitude of macroclimatic warming for each survey on each summit. We therefore derived the difference between the mean temperature during the 14 years prior to each survey and the mean temperature during a baseline period between 1900 to 1950, using data from the Climate Research Unit (CRU, version 4.06; *21*). We selected a 14-year time window for this analysis as it corresponds to two survey intervals and is consistent with the subsequent analyses presented below. Using the same type of generalized linear mixed-effects model as above, but exchanging time with the magnitude of warming as a fixed-effects predictor we found that local extinction rates were positively related to climate warming (estimate = 0.38±0.01/0.37±0.02/0.39±0.02 on the plot/summit/mountain region level, $p < 0.001$ in all cases, cf. table S5): with each additional 0.1°C of warming, the proportion of local extinctions has increased by 1.6%, 1.1%, and 1.0 % at the three levels of aggregation. This model explained a considerably higher proportion of the observed variance in local extinction rates (as measured by marginal R^2-values, $R^2m = 0.14/0.27/0.36 \pm 0.004/0.014/0.018$ on the plot/summit/ mountain region level) as compared to the model that used time as a fixed-effects predictor ($R^2m = 0.03/0.09/0.17 \pm 0.001/0.008/0.018$, cf. Fig. 3) which underpins the role of climate change in driving the increasing local extinction rates. Finally, to assess whether local extinction rates show geographical trends we also included latitude and longitude as additional fixed-effects predictors into the climate-warming model.

We found that at the plot, but not at the summit and region level, local extinction rates were higher at southern latitudes while there was no east-west gradient at any of the three aggregation levels (Fig. 3A and table S6).

Declining cover predicts local extinctions

To assess whether a species' decrease in local abundance can be considered an indicator of its local extinction risk, we computed the change in the observed cover between the first and the third survey for each species on each plot. A logistic mixed-effects model revealed that the likelihood that a species was reported as locally extinct at a plot during the fourth survey in 2022 indeed increased under stronger decline of cover of the focal species at this plot during the preceding 14 years (i.e., between 2001 and 2015, Fig. 3C, 4B and table S7). The effect was independent of the species' cover value in the first survey. The latter variable was itself a significant predictor of local extinction (Fig. 3C and table S7), most likely because low cover in the first survey increases the probability of both subsequent local extinctions and observation errors. Prior cover decline predicted local extinctions in the fourth survey also when computed over a shorter observation window of seven years, i.e., between the second and the third survey. However, the strength of the effect was weaker, probably because of stronger noise from random fluctuations (Fig. 3C, 4B and table S7).

The relationship between declining cover and local extinction rate was significant even though changes of cover prior to local extinction varied considerably in magnitude and direction, suggesting considerable background fluctuation. Of all local extinctions reported during the fourth survey, 57.6 % ± 0.2% were preceded by cover decline, 32.2% ± 0.2% by cover increase and 10.2% ± 0.1% by constant cover between the first and the third survey. To further support the conclusion that a declining cover leads to local extinction more often than expected by chance under this background fluctuation we counted all trajectories of monotonic cover decrease towards extinction across the four surveys, i.e., of type $cover_{survey1} > cover_{survey2} > cover_{survey3} > 0$. We then compared the number of such trajectories in the entire dataset to their number after randomly re-shuffling the cover values, including 0s, of each species at each plot across the four surveys. We found that these monotonic decline-to-extinction trajectories occurred 2.5 times more often than expected by chance (Fig. 4A, 44.5 ± 6.5 and 112.8 ± 2.7 trajectories for reshuffled and observed data, respectively), a difference that was highly significant (t-test, $d.f. = 1333209$, $p < 0.001$).

Species are more prone to local extinctions towards their lower range margin and in communities undergoing stronger thermophilization

If local extinctions of plant species on mountain summits are - at least partly - driven by the changing climate, we would expect that extinction risk is higher the closer a summit is located towards a species' warmer, lower range margin, in line with scattered recent observations in various mountain plant and animal species (*12, 22*). We tested this assumption based on a six-level classification of species according to the elevational belt where they most frequently occur (1 = nival; 2 = subnival or alpine-nival ecotone; 3 = alpine; 4 = alpine to the treeline; 5 = treeline ecotone; and 6 = montane *20*). We calculated the relative rank of each species in each plot as the average elevational rank of all species co-occurring in the plot (i.e., the community-mean value) in 2001 minus the species' elevational rank. This species-by-plot-specific value of relative elevational rank is hence an indicator of the position of the plot within the elevational range of a species. Positive values indicate that the "average species" of a plot prefers lower elevations than the focal species, suggesting that the plot is located towards the lower range margin of the focal species; and, vice versa, negative values indicate a location of the plot towards the upper elevational range margin of

the focal species. We added this relative elevational rank as a further predictor to the model used to analyse the relationship between local extinction probability in the fourth survey and cover change in the preceding 14 years. We found that the relative elevational rank was positively related to local extinction likelihood (Fig. 3C and table S7). Towards their lower elevational range margin, species hence had a higher risk of local extinction between 2015 and 2022. We moreover repeated the comparison of the 'decline-to-extinction trajectories' against random expectations, as described above, separately for local extinction events of species with positive and negative relative elevational ranks. We found that such trajectories occur more often than expected by chance in both groups, in line with a general impact of prior cover decline on local extinction likelihood. However, the overrepresentation was stronger for the group with positive elevational ranks, underlining that populations at lower range margins faced a higher risk of local extinction over time (Fig. 4A). Finally, we tested whether local extinctions in the fourth survey were more likely in communities undergoing a stronger general change towards warmth-demanding species (thermophilization, cf. *20*). We therefore calculated the change in the cover-weighted average elevational rank of plots between 2001 and 2022 (after removing the focal species, see 19 for details). We added this change as a predictor variable to the model and found that local extinctions between 2015 and 2022 were more likely in communities which experienced a stronger thermophilization (Fig. 3C, table S7). This finding underlines that local extinctions are, at least partly, embedded into a climate-driven restructuring of the entire community.

Discussion

Monitoring plant occurrence and cover on permanent plots is prone to observer error (*23*). Although relocation errors are minimized by the permanent-plot design of GLORIA, and identification errors were reduced as much as possible by prior data cleaning (see 19), part of the local extinctions reported certainly result from species that were overlooked or from natural fluctuation. However, if all local extinctions were attributable to observer errors or random fluctuation, significant relationships with time, level of warming, or relative elevational rank should not emerge. In fact, the explanatory power of our models (marginal R^2-values reached up to 0.75, see Fig. 3 and tables S6 and S7) demonstrate that these variables explain a high proportion of the observed variation in local extinction rates. Moreover, transitions suggesting real local extinctions increased over time and monotonic decline-to-extinction trajectories were far more frequent than expected by chance. Finally, a complementary analysis of colonization dynamics, mirroring our analyses of extinction dynamics, further suggests that the data do not exclusively reflect natural fluctuation and observer error (see 19 for details). In particular, this complementary analysis demonstrated that, in correspondence with the patterns found for local extinctions, a monotonic increase of a species' cover following local colonization (i.e. a transition of type $0 < \text{cover}_{\text{survey2}} < \text{cover}_{\text{survey3}} < \text{cover}_{\text{survey4}}$) was much more likely than expected under random fluctuations; and that local colonizations were significantly more frequent towards the species upper elevational range limits. However, in contrast to extinctions, colonizations did not become more frequent over time. Finally, the number of colonization events were also unrelated to the level of warming, most likely because of their strong dependence on the availability of potential colonizers in the plots' immediate surroundings (36, 39).

While our results indicate a significant impact of climate change on rising local extinction rates, we cannot exclude additional effects due to other anthropogenic drivers. In the case of GLORIA, strong impacts of land-use changes are unlikely because summits were selected with the explicit purpose of minimizing land-use changes (*17*). A possible effect of

atmospheric nitrogen deposition (*12*) remains to be tested, even if an earlier study based in part on GLORIA data, did not detect any consistent impact of nitrogen deposition on local plant species richness of European mountain summits (*2*). Besides these non-climatic factors, climate-related changes other than warming temperatures could foster extinction rates, especially decreasing water availability and a shortened snow cover period (*13, 24*). Robust data on how these factors have developed across GLORIA summits are not available and their impact cannot hence be disentangled from the one of warming yet. However, changes in these factors are likely correlated with higher temperatures as the latter increase evaporative demand (*25*), shift the ratio of rain and snow (*26*) and advance spring snowmelt (*27, 28*). We hence emphasize that the demonstrated link between the exposure to climate warming and local extinction rates does not necessarily indicate an impact of temperature *per se*, but rather reflects a response to a set of conditions altered by rising temperature. These changes may also include alterations of the biotic environment. Indeed, the combination of rising species numbers, increasing total vegetation cover (Fig. 3B, table S3 and S4) and community thermophilization may indicate that increasing competitive pressure has already contributed to the rise of local extinction events (*29, 30*). Such competitive effects would be in line with the widely accepted hypothesis that the climatically more favourable range margins, where we found extinctions to be more frequent, are primarily set by competitive interactions (*31-34*). However, a conclusive distinction of direct and indirect effects of climate change on local extinctions can only be confirmed through experiments (*29*).

In summary, our results show that climate change does not only add additional species to European summit floras (*2, 4*) but also causes loss of former residents, and that local extinctions are more frequent towards the species' lower range margin. As a consequence, the species characteristic of the highest elevations will also face highest extinction risk because they have least opportunities to offset lower-margin losses by upper-margin expansion. The focus on the salient biodiversity increase has masked simultaneous extinctions to a certain extent, and the latter have received more attention only over the most recent years (*13, 14, 35, 36*). This may reflect the fact that local extinctions are intrinsically more difficult to demonstrate than local colonizations. The recent rise of attention on extinctions may, however, also suggest that climate-driven local extinctions happen more slowly than colonizations, which is likely in the case of long-lived and stress-tolerant alpine plants (*37-39*). This is consistent with the rising number of local extinction events detected here and might imply that an extinction debt, accumulated since at least the most recent amplification of climate change during the 1980s (*40*), is now starting to become paid off.

References and Notes

1. G. Grabherr, M. Gottfried, H. Pauli, Climate effects on mountain plants. *Nature* **369**, 448 (1994).
2. M. J. Steinbauer *et al.*, Accelerated increase in plant species richness on mountain summits is linked to warming. *Nature* **556**, 231-234 (2018).
3. N. Pepin *et al.*, Elevation-dependent warming in mountain regions of the world. *Nature Climate Change* **5**, 424-430 (2015).
4. H. Pauli *et al.*, Recent plant diversity changes on Europe's mountain summits. *Science* **336**, 353-355 (2012).
5. Y. Telwala, B. W. Brook, K. Manish, M. K. Pandit, Climate-induced elevational range shifts and increase in plant species richness in a Himalayan biodiversity epicentre. *PloS one* **8**, e57103 (2013).
6. S. Wipf, V. Stöckli, K. Herz, C. Rixen, The oldest monitoring site of the Alps revisited: accelerated increase in plant species richness on Piz Linard summit since 1835. *Plant Ecology & Diversity* **6**, 447-455 (2013).
7. I. R. Staude *et al.*, Directional turnover towards larger-ranged plants over time and across habitats. *Ecology Letters* **25**, 466-482 (2022).

8. D. Mouillot *et al.*, Rare species support vulnerable functions in high-diversity ecosystems. *PLoS biology* **11**, e1001569 (2013).
9. S. G. Flantua *et al.*, Snapshot isolation and isolation history challenge the analogy between mountains and islands used to understand endemism. *Global Ecology and Biogeography* **29**, 1651-1673 (2020).
10. T. Dirnböck, F. Essl, W. Rabitsch, Disproportional risk for habitat loss of high-altitude endemic species under climate change. *Global Change Biology* **17**, 990-996 (2011).
11. Y. Chauvier-Mendes *et al.*, Transnational conservation to anticipate future plant shifts in Europe. *Nature Ecology & Evolution* **8**, 454-466 (2024).
12. S. B. Rumpf *et al.*, Range dynamics of mountain plants decrease with elevation. *Proceedings of the National Academy of Sciences* **115**, 1848-1853 (2018).
13. A. Lamprecht, P. R. Semenchuk, K. Steinbauer, M. Winkler, H. Pauli, Climate change leads to accelerated transformation of high-elevation vegetation in the central Alps. *New Phytologist* **220**, 447-459 (2018).
14. K. Steinbauer, A. Lamprecht, P. Semenchuk, M. Winkler, H. Pauli, Dieback and expansions: Species-specific responses during 20 years of amplified warming in the high Alps. *Alpine Botany* **130**, 1-11 (2020).
15. C. McCain, T. Szewczyk, K. Bracy Knight, Population variability complicates the accurate detection of climate change responses. *Global Change Biology* **22**, 2081-2093 (2016).
16. A. Futschik *et al.*, Disentangling observer error and climate change effects in long-term monitoring of alpine plant species composition and cover. *Journal of Vegetation Science* **31**, 14-25 (2020).
17. H. Pauli *et al.*, *The GLORIA field manual: standard multi-summit approach, supplementary methods and extra approaches*. (GLORIA-Coordination, Austrian Academy of Sciences & University of Natural …, 2015).
18. H. Pauli, S. R. Halloy, in *Oxford Research Encyclopedia of Climate Science*. (2019).
19. Materials and methods are available as supplementary materials.
20. M. Gottfried *et al.*, Continent-wide response of mountain vegetation to climate change. *Nature climate change* **2**, 111-115 (2012).
21. I. Harris, T. J. Osborn, P. Jones, D. Lister, Version 4 of the CRU TS monthly high-resolution gridded multivariate climate dataset. *Scientific data* **7**, 109 (2020).
22. S. B. Rumpf, K. Hülber, N. E. Zimmermann, S. Dullinger, Elevational rear edges shifted at least as much as leading edges over the last century. *Global Ecology and Biogeography* **28**, 533-543 (2019).
23. N. W. Mason, R. J. Holdaway, S. J. Richardson, Incorporating measurement error in testing for changes in biodiversity. *Methods in Ecology and Evolution* **9**, 1296-1307 (2018).
24. P. Niittynen, R. K. Heikkinen, M. Luoto, Snow cover is a neglected driver of Arctic biodiversity loss. *Nature Climate Change* **8**, 997-1001 (2018).
25. S. Sherwood, Q. Fu, A drier future? *Science* **343**, 737-739 (2014).
26. A. Gobiet *et al.*, 21st century climate change in the European Alps—A review. *Science of the total environment* **493**, 1138-1151 (2014).
27. S. B. Rumpf *et al.*, From white to green: Snow cover loss and increased vegetation productivity in the European Alps. *Science* **376**, 1119-1122 (2022).
28. P. Choler, A. Bayle, N. Fort, S. Gascoin, Waning snowfields have transformed into hotspots of greening within the alpine zone. *Nature Climate Change* **15**, 80-85 (2025).
29. J. M. Alexander, J. M. Diez, J. M. Levine, Novel competitors shape species' responses to climate change. *Nature* **525**, 515-518 (2015).
30. C. Rixen *et al.*, Intraspecific trait variation in alpine plants relates to their elevational distribution. *Journal of Ecology* **110**, 860-875 (2022).
31. R. H. MacArthur, *Geographical ecology: patterns in the distribution of species*. (Princeton University Press, 1984).
32. J. H. Connell, Diversity in tropical rain forests and coral reefs: high diversity of trees and corals is maintained only in a nonequilibrium state. *Science* **199**, 1302-1310 (1978).
33. J. Leathwick, M. Austin, Competitive interactions between tree species in New Zealand's old-growth indigenous forests. *Ecology* **82**, 2560-2573 (2001).
34. J. Lenoir *et al.*, Going against the flow: potential mechanisms for unexpected downslope range shifts in a warming climate. *Ecography* **33**, 295-303 (2010).
35. M. Varricchione, M. L. Carranza, V. Di Cecco, L. Di Martino, A. Stanisci, Warmer and poorer: the fate of Alpine calcareous grasslands in Central Apennines (Italy). *Diversity* **14**, 695 (2022).
36. N. Helm *et al.*, Fine-scale alpine plant community assembly: Relative roles of environmental sorting, dispersal processes and species interactions. *Journal of Ecology* **112**, 2745-2757 (2024).
37. S. T. Jackson, D. F. Sax, Balancing biodiversity in a changing environment: extinction debt, immigration credit and species turnover. *Trends in ecology & evolution* **25**, 153-160 (2010).

38. S. Dullinger *et al.*, Extinction debt of high-mountain plants under twenty-first-century climate change. *Nature climate change* **2**, 619-622 (2012).
39. J. M. Alexander *et al.*, Lags in the response of mountain plant communities to climate change. *Global change biology* **24**, 563-579 (2018).
40. P. C. Reid *et al.*, Global impacts of the 1980s regime shift. *Global change biology* **22**, 682-703 (2016).
41. J. Wessely *et al.*, Data and code for the manuscript: "Rising plant extinction rates on European mountain summits". Dryad. https://doi.org/10.5061/dryad.vmcvdnd6v
42. R. Kindt, WorldFlora: An R package for exact and fuzzy matching of plant names against the World Flora Online taxonomic backbone data. *Applications in Plant Sciences* **8**, e11388 (2020).
43. S. J. Smith, J. Edmonds, C. A. Hartin, A. Mundra, K. Calvin, Near-term acceleration in the rate of temperature change. *Nature Climate Change* **5**, 333-336 (2015).
44. D. Bates, M. Mächler, B. Bolker, S. Walker, Fitting linear mixed-effects models using lme4. *Journal of statistical software* **67**, 1-48 (2015).
45. A. Kuznetsova, P. B. Brockhoff, R. H. Christensen, lmerTest package: tests in linear mixed effects models. *Journal of statistical software* **82**, 1-26 (2017).
46. K. Bartoń, MuMIn: multi-model inference., (2025).
47. R Core Team. (R Foundation for Statistical Computing, Vienna, Austria, 2023).
48. M. McGillycuddy, DI. Warton, G. Popovic, BM. Bolker, Parsimoniously Fitting Large Multivariate Random Effects in glmmTMB." *Journal of Statistical Software*, **112**(1), 1–19, (2025).
49. D. Lüdecke, M. S. Ben-Shachar, I. Patil, P. Waggoner, D. Makowski, performance: An R package for assessment, comparison and testing of statistical models. *Journal of open source software* **6**, (2021).

Acknowledgments:

Funding:

European Research Council (ERC) under the European Union's Horizon 2020 research and innovation program (ERC-Adv grand MICROCLIM, Grant Agreement No. 883669). JB received additional funding from the Department of the Environment of the Regional Government of Aragon (Spain) and Ordesa and Monte Perdido National Park. SW received additional funding from the Swiss Federal Office for the Environment (FOEN) Dr. Joachim de Giacomi foundation Research Commission of the Swiss National Park Office for Nature of the Canton of Grisons. TV received additional funding from the Research Foundation - Flanders (FWO, no. 1268126N).

Author contributions:

Conceptualization: SD, JW

Methodology: JW, SD, KH

Investigation: JW, SD

Visualization: JW, SD, DM

Data acquisition: OA, CA, EB, DB, JB, RB, MC, PC, VC, PC, JD, RF, PF, MG, DG, KG, BG, AH, JJ, KK, RK, JK, AL, JL, JL, JL, PN, MP, CR, CR, GR, PS, TU, TV, MV, PV, MW, SW, HP

Writing – original draft: SD, JW

Writing – review & editing: JW, KC, AG, JH, NH, KH, DM, OA, CA, EB, DB, JB, RB, MC, PC, VC, PC, JD, RF, PF, MG, DG, KG, BG, AH, JJ, KK, RK, JK, AL, JL, JL, JL, PN, MP, CR, CR, GR, PS, TU, TV, MV, PV, MW, SW, HP, SD

Competing interests:

Authors declare that they have no competing interests.

Data and materials availability:

459 The data that support the findings of this study is available online in the Dryad database. All
460 code used for the analysis as well as for producing the figures is available online in the Dryad
461 database (41).
462

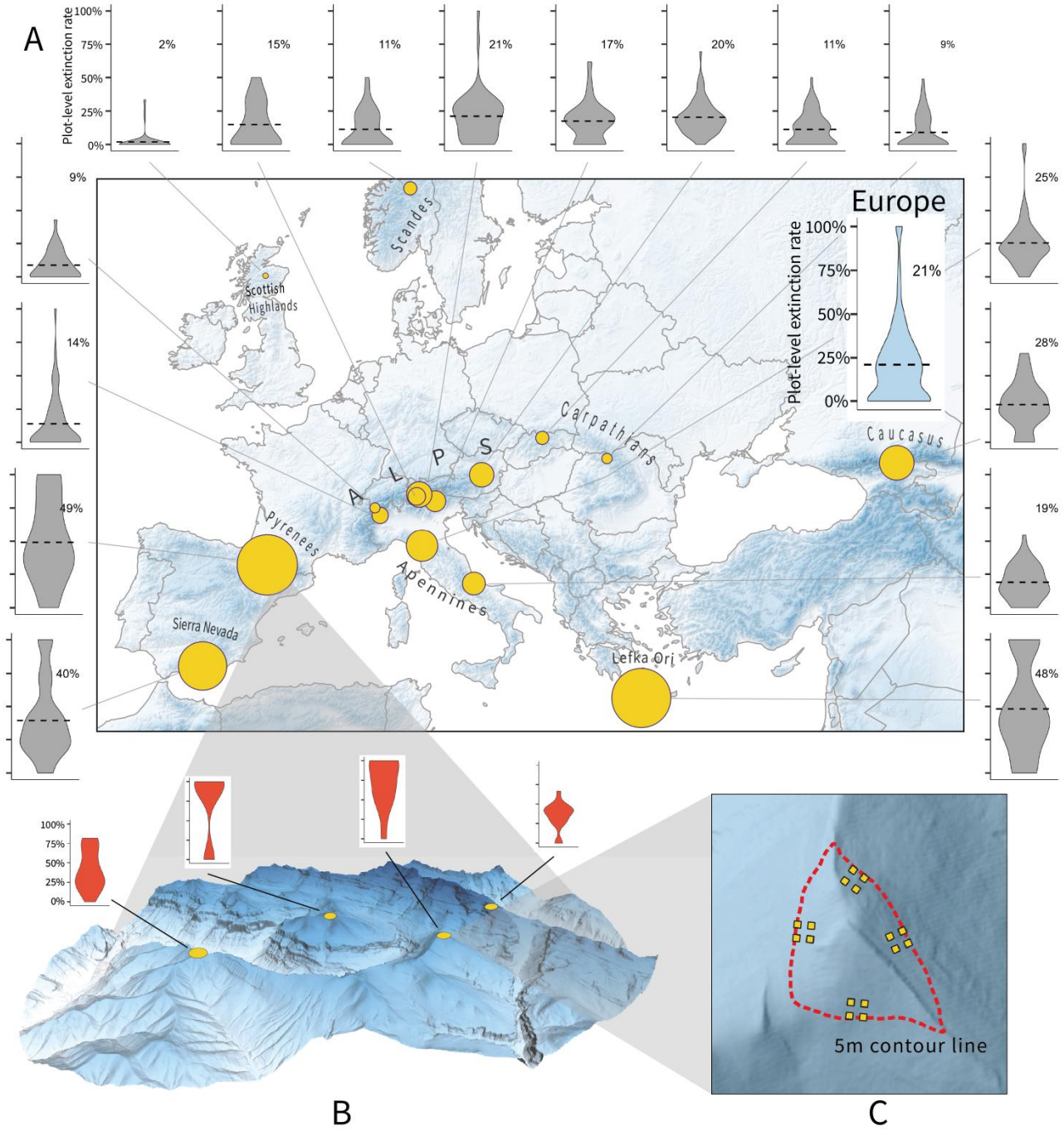

Fig. 1: Local extinction rates on European mountain summits. A) Geographical distribution of the 16 mountain regions surveyed. The size of the circles represents the mean proportion of local extinctions from 2001 to 2022, i.e., of species observed in 2001, but not re-observed in 2022, across all plots of a given mountain region. The violin plots show the distribution of the plot-wise extinction rates (% per plot) across Europe (blue), within each mountain region (grey) [as well as within each summit in the Pyrenees in panel B (red)]. Dashed lines show the mean extinction rate across all plots in the respective region or across Europe. B) Each mountain region comprises three to four summits as exemplified for the Pyrenees. C) On each summit, up to 16 plots (yellow squares) are permanently installed, arranged in four plot clusters in each cardinal direction 5 meters below the peak (the respective contour line is depicted as dashed red line).

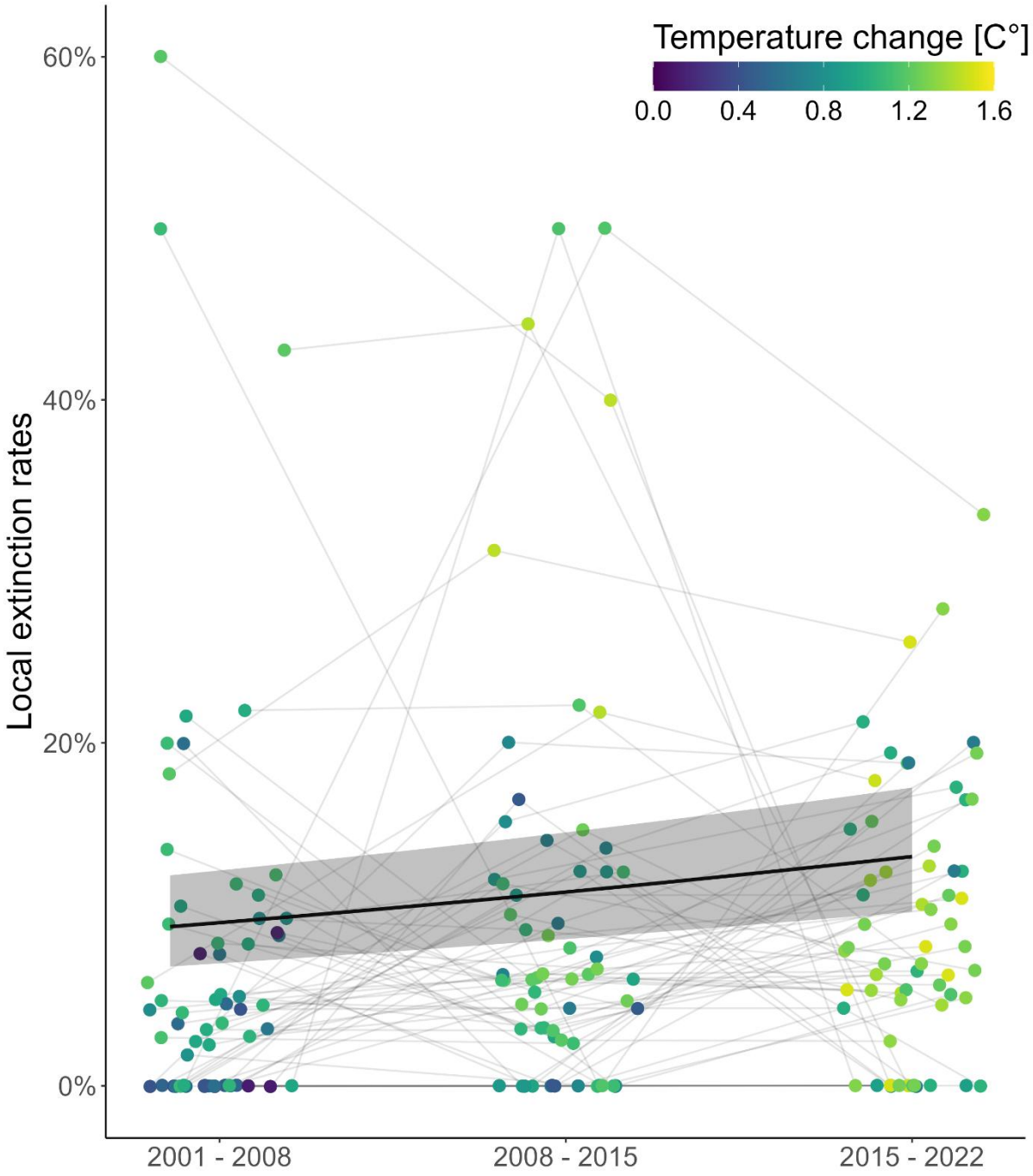

Fig. 2: Local extinctions increased across surveys. Values on the y-axis represent the percentage of species observed in one but not re-observed in the consecutive survey on the same summit (each dot represents one of the 62 summits analysed). Dot colour represents the temperature change in the 14 years before the respective time interval, compared to a summit-specific baseline climate of the years 1900 to 1950. The regression line is the fixed effect of a generalized linear mixed-effects model for the proportion of local extinctions against time ($p < 0.001 \pm 0.000$, $R^2m = 0.09 \pm 0.008$, $R^2c = 0.73 \pm 0.011$). The grey band indicates the 95% confidence interval. All values, i.e., percentage of local extinctions as well as the regression line, are the mean of 1000 resamples. The grey lines link the dots representing one particular summit.

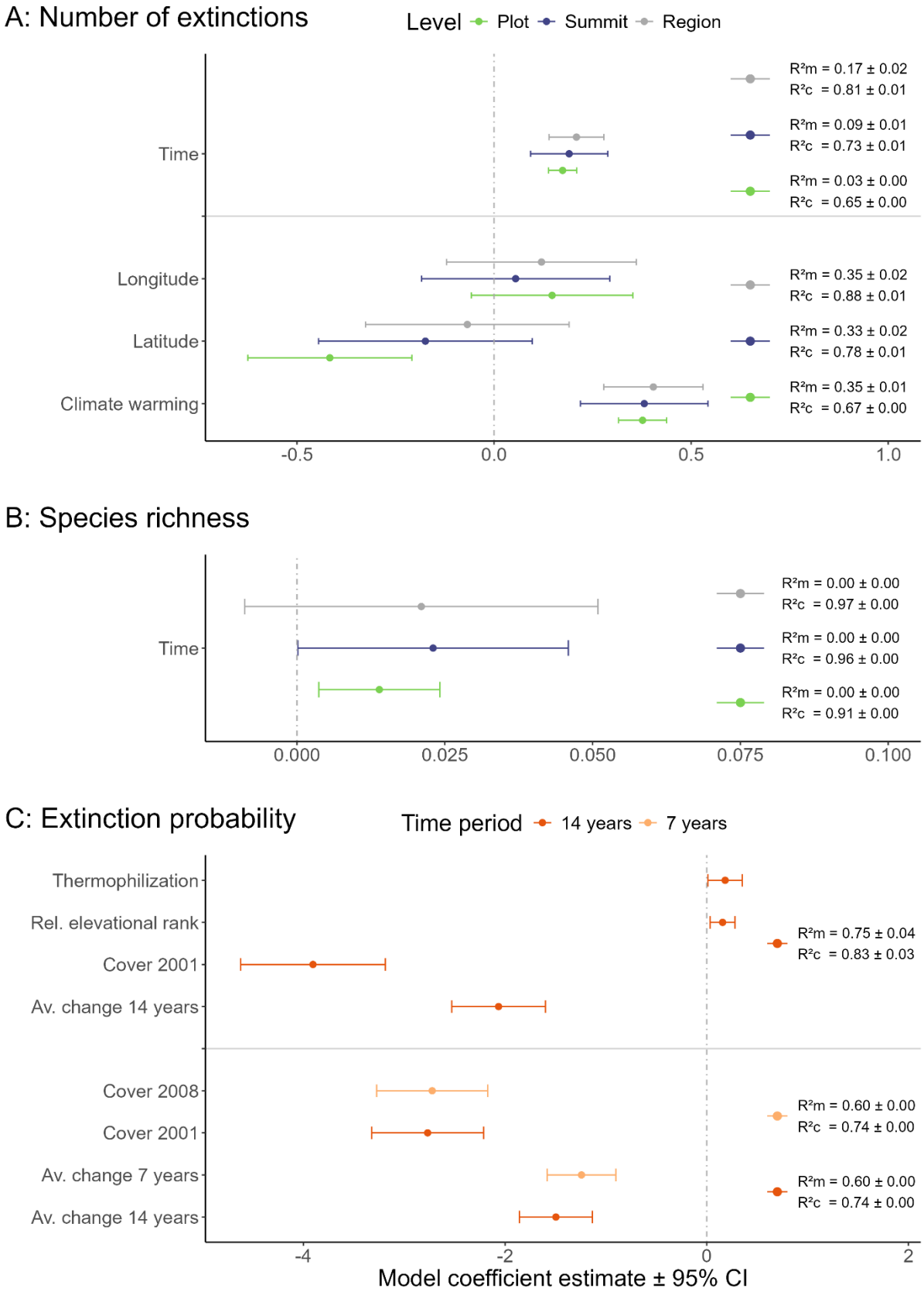

Fig. 3: Extinction probability increases with stronger warming, for species of higher elevation and after longer phases of decline. Panels show mean model coefficients (of 1000 resamples) of linear mixed-effects models and their 95% confidence interval (CI).

Confidence intervals not overlapping with 0 indicate significant fixed effects. Mean marginal (m) and conditional (c) R^2 values and their standard deviation were also derived from the 1000 resamples. The following models are illustrated: A) Generalized linear mixed-effects models for proportion data with the proportion of extinctions, as response and time (upper part of the panel) or climate warming, latitude and longitude as fixed effects (lower part) at the plot (green), summit (blue) and mountain region (grey) level. B) Generalized linear mixed-effects models for count data with the total species number as response and time as fixed effect at the plot (green), summit (blue) and mountain region (grey) level. C) Logistic mixed-effects models with local extinction (yes/no) as response and average cover change per year between the first or second and the third survey (representing a period of approximately 7 or 14 years, orange and dark red), and the cover at the beginning of the respective period as fixed effects. Negative estimates imply increased extinction risk for lower cover values as well as for stronger cover decreases. In the model represented in the upper part of the panel relative elevational rank and thermophilization are used as additional fixed effects All predictors were scaled to zero mean and unit variance.

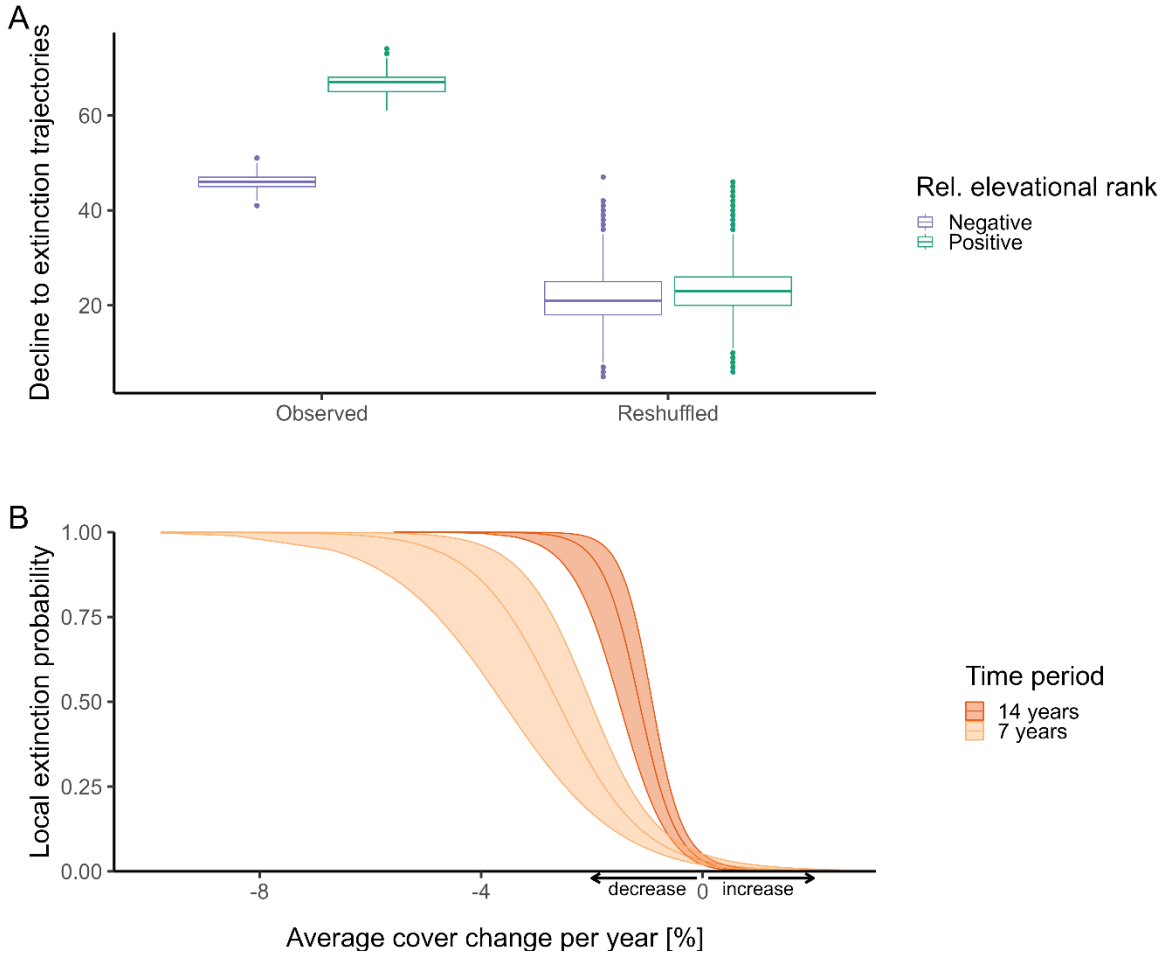

Fig. 4: Preceding change in cover is related to the probability of species' extinction. A) Number of trajectories of monotonic cover decrease during the first three surveys, followed by extinction in the fourth one ($cover_{survey1} > cover_{survey2} > cover_{survey3} > 0$) in the observed data and after randomly re-shuffling species cover values on each plot across the four surveys 100 times. The comparison was done separately for species with negative and positive relative elevational ranks, indicating a position of the monitoring plot towards the upper or lower range margin of the species, respectively. Boxplots represent the variation across 100

reshuffles of 1000 resamples from the data. For both groups the difference between the observed and reshuffled data was highly significant (t-tests, *d.f.* = 1266957/1390299, $p < 0.001$). B) The relationship between preceding cover change per year and the probability of a species to go extinct in a plot, i.e., to be not re-detected in the fourth survey. Results of two logistic mixed-effects models with local extinction (yes/no) as response variable and a random intercept for summit nested in mountain region, as well as a random intercept for species. Fixed effects were the average cover change per year between the first or second and the third survey covering a period of approximately 7 and 14 years, respectively, and the cover at the beginning of the respective period. Shaded areas represent 95% confidence intervals, averaged across 1000 resamples from the data. All predictors were scaled to zero mean and unit variance.

Supplementary material:

Materials and Methods

Species observations

In 2022, GLORIA-Europe (*20*), the largest systematic monitoring initiative of climate impacts on high-mountain vegetation, conducted its fourth round of surveys of 896 monitoring plots distributed across 62 summits in 16 mountain regions across Europe. The initial survey and subsequent resurveys were conducted in the years 2001, 2008, 2015 and 2022 with some slight deviations in some mountain regions (see table S8 for detailed information). Monitoring plots were established on four summits per mountain region (or three summits in one of the regions), with summit heights ranging from the treeline to the highest elevations represented in the respective mountain range. On each summit, 16 vegetation plots (less in a few cases due to topographical constraints, see table S7 for detailed information) of 1 m × 1 m each were permanently installed (see Figure 1), four per cardinal direction (from here on called plot clusters). In each of the four surveys all vascular plant species and their cover (visual estimation in %, down to 0.005 %) in these plots were recorded. Additionally, each plot was subdivided into 100 subplots of 10 cm × 10 cm and the presence of all vascular plant species was recorded in each subplot. This method to assess frequency was consistently applied across all plots during the first and second survey, across 693 of the 896 initial plots during the fourth survey, but was omitted during the third survey. Here, we analysed local extinction events of species within survey intervals defined as observation of species in one, followed by lack of observation in the subsequent survey. Analyses were computed separately at the plot, summit and mountain region level and focused on all observed local extinctions in assessments of spatial and temporal trends, but only on species present in the initial survey in 2001 when analysing the possible effect of prior decline on local extinctions reported in 2022 (see below for details).

Species taxonomy was standardised using the *WorldFlora* package in R (*42, version v.2022.12*). For species marked as unchecked (by the package), names were defined using Plants of the World Online (https://powo.science.kew.org/).

Data cleaning and accounting for uneven sampling efforts

Misidentifications of the same species as different taxa in different surveys may bias local extinction rates towards higher values. To be conservative in this respect, we removed entries where one species was not re-observed but another species of the same genus colonized a particular plot in the same survey (4.6% of all species × plot combinations). Species of the genera *Alchemilla, Euphrasia, Hieracium, Pilosella* as well as *Taraxacum* were additionally removed due to potential identification issues.
Applying or not applying the frequency method during sampling has potential implications for the number of species observed in a plot, and hence also for (apparent) local extinctions, because this method increases the time spent per plot, and hence sampling effort, considerably. To estimate this effect, we compared plots monitored with and without the frequency method in the same plot cluster during the fourth survey and indeed found a higher detection probability of species when the frequency method was applied. We therefore corrected the number of local extinctions in combinations of plot and survey in which the frequency method was not applied. To do so, we compared the recolonisation rates from the third to the fourth survey (i.e., the percentage of species present on a plot in the second survey, considered extinct in the third survey, but re-observed in the fourth) between plots

with and without the application of the frequency method in the fourth survey. The comparison was done via a one-sided paired t-test pairing plots of the same plot cluster surveyed with and without the frequency method in the fourth survey. We found that recolonisation rates for plots where the frequency method was applied during the fourth survey were on average 12.1% higher ($p = 0.026$) indicating that 12.1 % of apparent extinctions during the third survey, resulted from species overlooked due to lower sampling effort. To correct for this uneven sampling effort, we randomly chose 12.1% of all species that were not re-observed in a plot and set their cover to 0.1% in the respective plot. We did this for all plots in the third survey and for the 217 plots where the frequency method was not applied during the fourth survey. We therefore drew from a binomial distribution with a probability of success of 0.121 for each species that was not re-observed in a plot. For all species for which we drew a one in this process the cover was corrected. This random sampling was repeated 1000 times, and all further analyses were done for all 1000 resamples separately. Finally, for all results we derived means and standard deviations of the models of all resamples.

Computation of warming rates

Monthly average temperatures from 1900 to 2022 were extracted from the Climate Research Unit (CRU, version v4.06) dataset (*21*). As the native spatial resolution of this dataset is rather coarse (0.5 arcsec), it was further statistically downscaled to a 100 m resolution using the delta method (*38*). For each survey and each summit, climate warming was derived as the difference between the mean temperature of the 14-years period preceding a survey and the mean temperature of the time 1900 to 1950, a period before the onset of more rapid recent anthropogenic climate change (*43*). We used a period of 14 years for this analysis because it corresponds to the duration of two monitoring intervals, which we also used to explore the relationship between local extinctions and preceding abundance decline (see below).

Statistical analyses

The relationship between the proportion of local extinctions at the plot, summit and mountain region level and time as well as exposure to climate warming and geographical position was tested using separate generalized linear mixed-effects models (GLMMs). We built GLMMs for proportion data with the number of local extinctions (= species observed in the first, but not in the consecutive survey, as success) and the number of local persistences (= species observed in two consecutive surveys, as failures) per time interval on all three levels of spatial aggregation as a two-column response variable. Year of sampling was included as a numeric predictor in the fixed effects of the model and random intercepts were used for plot nested in summit nested in mountain region, summit nested in mountain region, or mountain region alone, depending on the level of spatial aggregation we used in the analysis (i.e., plot, summit or mountain region level, respectively). In a second model of the same type, we used the exposure to climate warming per summit, tailored to each time interval (see *Computation of warming rates* above), first alone and then combined with geographical longitude and latitude, as predictors in the fixed effects of the model and random intercepts, again for plot nested in summit nested in mountain region, summit nested in mountain region, or mountain region alone, depending on the level of spatial aggregation (i.e., plot, summit or mountain region level, respectively). For all models, predictors were scaled to zero mean and unit variance. To derive the increase of local extinction rates under additional warming of 0.1°C, we used the latter model (with exposure to climate warming as the only predictor) to predict the local extinction rates (fixed effects only) under average climate warming across all

summits of the average conditions between 2001 and 2015 (+1.2°C) as well as under additional 0.1°C (i.e., +1.3°C).

To better distinguish background dynamics (due to observation error or due to natural fluctuation of species presence), from real extinction dynamics, we focused on two specific types of transitions for each combination of species and plot, summit or region: the first of type presence-absence-presence (1-0-1) represents background dynamics whereas the second of type presence-absence-absence (1-0-0) was interpreted as indication of real extinctions. To test whether the probability of these two types of transitions has increased from the first window of three surveys (2001 – 2008 – 2015) to the second one (2008 – 2015 – 2022), we used two GLMMs for proportion data with the number of either 1-0-1 or 1-0-0 trajectories as success and the number of trajectories starting with presence and following other transition patterns than the focal one as failures. The fixed-effects predictor was the survey window and the random-effects structure was the same as described above.

To analyse the relationship between species richness and time at the plot, summit and mountain region level, we used GLMMs for count data (assuming a Poisson error distribution) that were checked for overdispersion. Year of sampling was included as a numeric predictor in the fixed effects of the model and random intercepts were used in the same way as in the models described above.

The relationship between local extinction probability and preceding cover changes was analysed at the species-by-plot level using a logistic mixed-effects model (i.e., the response variable is binary: 1 or 0 for species local extinction or persistence, respectively) with a random intercept term for summit nested in mountain region as well as an additional random intercept term for species. To evaluate if the relationship between local extinctions and cover change strengthens if longer observation periods for cover change are used, we build two different models. The fixed-effects predictors were, for the first model, the average cover change per year between the first and the third survey (a 14-year period in most cases) as well as the cover during the first survey. For the second model, the fixed-effects predictors were the average cover change per year between the second and the first survey (a 7-year period in most cases) as well as the cover during the second survey. All fixed-effects predictors were scaled to zero mean and unit variance. To obtain a fair comparison (i.e., the same sample size for both models) we analysed only local extinctions between the third and fourth survey, making sure that species were present in all preceding surveys.

Additionally, we tested if local extinction probability differed depending on whether a species is more characteristic of, in relative terms (i.e., compared to the other species co-occurring in the same focal plot), higher or lower elevations. Therefore, we used elevational ranks that had been assigned to all species by regional experts, mostly those who also conducted the surveys. The ranks indicate the elevational belt within which the species has its center of distribution and were coded as: 1 = nival; 2 = subnival, i.e., at the transition between the upper alpine and lower nival belt; 3 = alpine; 4 = alpine to the treeline; 5 = treeline ecotone; and 6 = montane (*20*). For each species and each plot, we computed the difference between the average elevational rank at the community level (i.e., the community mean of all species' elevational rank values) of the plot during the first survey and the elevational rank of the focal species. We interpreted this difference as an indicator of the position of the plot within the elevational interval covered by the focal species. The rationale of the latter is that a species with an elevational rank higher (= numerically lower) than the average of the community is likely occurring at a plot located lower than where it is usually found, hence towards its lower range margin. Subsequently, this relative elevational rank was included into

the model relating local extinction rates to the cover during the first survey and the cover change between the first and third survey.

To explore whether local extinctions in the last survey align with a broader, climate-driven re-structuring of communities we further used these elevational ranks to compute thermophilization of communities between the first and the last survey. Thermophilization is defined as the change in the cover ratio of warmth-demanding to cold-adapted species within a community (*20*). We therefore calculated the average elevational rank of each community in the first and last survey, but this time as a weighted average, with weights set according to species' cover values. As we wanted to use this variable as an additional potential predictor of local extinction, we did these calculations after prior removal of the focal species to avoid circularity. Put differently, each trajectory of a species on each plot was associated with the change in the cover-weighted average elevational rank of all other, co-occurring species on the plot between the first and the last survey. We then added this variable to the model relating the probability of local extinction between the third and fourth survey to the cover during the first survey, the cover change between the first and third survey, and the relative elevational rank of the species.

Finally, to provide additional support that the trajectories of decline and eventual extinction in our data are more frequent than expected under background dynamics (including observer errors) we counted the clearest such decline-to-extinction trajectories, i.e., those with a monotonic decline from the first to the third survey and an extinction in the fourth one (i.e., of type $over_{survey1} > cover_{survey2} > cover_{survey3} > 0$). We subsequently re-shuffled the species cover values, including 0, across the four surveys randomly 100 times for each of the 1000 random samples accounting for the uneven sampling effort (see above) and re-counted the then emerging trajectories of this type. We did this for all species together, but also separately for the subgroup of species with elevational ranks higher and lower than the average species of the community. We compared, by means of two-sample t-tests, numbers from the empirical dataset with numbers obtained after randomly re-shuffling species cover values.

Complementary analysis of colonization dynamics

Although our paper is focused on studying local extinctions, we additionally analysed local colonizations as well, to provide a complete picture of observed species dynamics. We thereby concentrated on analyses that are sensible correlates of those we conducted for local extinctions. In particular, we computed the number of local colonization events observed per resurvey and analysed their relationship with time and exposure to climate change. We repeated the analyses aiming at a better distinction between background dynamics (due to observation error or natural fluctuation of species presence) and real local colonization events; and we assessed whether local colonizations were more likely towards the upper range margins of species, in analogy to local extinctions supposedly more likely towards the species' lower range margins. We briefly document the corresponding methods and results here.

Regarding methods we tried to use the same statistical approaches as in the analyses of local extinctions, but with some necessary modifications. First, we had analysed local extinctions via binomial GLMMs because there is a clear distinction between success (species observed at a site in one survey, but not in the subsequent one) and failure (species observed in both surveys). However, in case of local colonizations, the data only deliver information about successes but not about failures, i.e., we can count the colonization events (species observed at a site in one survey, but not in the previous one) but we lack data on how many species could have colonized the plot but did not do so. Instead of binomial GLMMs we hence used

negative binomial GLMMs with the number of local colonizations as the response variable to study the relationship of local colonizations with time and exposure to warming. With respect to all other settings, the statistical models were built in the same way as those we had used for local extinctions, i.e., the predictors were year of sampling or exposure to climate warming per summit, tailored to each time interval (see *Computation of warming rates* above), and random intercepts were used for plot nested in summit nested in mountain region, summit nested in mountain region, or mountain region alone, depending on the level of spatial aggregation we used in the analysis (i.e., plot, summit or mountain region level, respectively). For all models, fixed-effects predictors were scaled to zero mean and unit variance. No model showed overdispersion nor zero inflation as checked using the *performance* package.

For fitting models analogous to those used for better distinction of background dynamics and extinction dynamics in the case of colonization dynamics, we separately compared transitions of type absence-presence-absence and of type absence-presence-presence between the earlier (2001-2008-2015) and later (2008-2015-2022) three surveys. We interpreted the first sequence as an indication of background dynamics and the latter as indication of real local colonization events. We again used a negative binomial GLMM with the number of such sequences in the two time-windows as the response and the identity of this time-window as the fixed-effect predictor variable, with random intercepts as described in the previous paragraph.

In further analogy with the extinction analysis, we investigated if local colonizations are followed by increasing cover more often than expected by chance under the given background fluctuation. We therefore counted all trajectories of monotonic cover increase after local colonization across the four surveys, i.e., of type $0 < cover_{survey2} < cover_{survey3} < cover_{survey4}$. We then compared the number of such trajectories in the entire dataset to their number after randomly re-shuffling the cover values, including 0s, of each species at each plot across the four surveys.

For evaluating whether colonization events occur significantly more often towards the upper range limits of a species we again computed the difference between the average elevational rank (i.e., the community mean of all species' rank values) of the plot during the first survey and the elevational rank of the focal, colonizing species. To keep the analogy with the analysis of local extinctions only colonization events of species that were not present on the focal plot in the first survey, but still present in the last re-survey were included in this analysis. Again, positive values indicate that the species mainly occurs at elevations higher than the average species within the plot and thus a location of the plot towards the lower elevational margin of a species range; and, vice versa, negative values indicate that the species mainly occurs at elevations lower than the average species within the plot and hence a location of the plot towards the upper elevational range margin of the species. As we lacked information about failures (see explanation above), we used an intercept-only model in this analysis, i.e., we evaluated whether the relative elevational rank of colonizing species is lower than zero using a linear mixed-effects model with random effects according to the level of spatial aggregation as described above.

The results of these analyses demonstrate that local colonization events were even more frequent than local extinction events in the earlier resurveys, and approximately as frequent as local extinctions in the latest one: across the three re-surveys, their number varied as follows: 1391 to 1401 ± 6 at the plot level; 189 to 194 at the summit level; and 95 ± 1.45 to 102 at the mountain region level (see table S9). In contrast to local extinctions, the number of colonization events did not change significantly with time nor with exposure to climate change, on none of the three levels of spatial aggregation (see table S10 and S11). Consistent

with these results, neither the transitions of type absence-presence-absence nor those of type absence-presence-presence became more frequent between the earlier (2001-2008-2015) and later (2008-2015-2022) three surveys. However, monotonic thrive-after-colonization trajectories (= of type $0 < cover_{survey2} < cover_{survey3} < cover_{survey4}$) occurred 3.0 times more often than expected by chance (44.5 ± 6.5 and 133.2 ± 1.4 trajectories for reshuffled and observed data, respectively), a difference that was highly significant (t-test, *d.f.* = 1096473, $p < 0.001$) – a finding that indicates that many of the observed local colonizations were real and followed by establishment of the species in the local community. Finally, colonizing species had indeed a significantly higher elevational rank (= subtraction of their elevational rank from the community-level mean resulted in a negative value) than the resident community, suggesting that colonizers are mainly coming from below and/or colonization events predominantly occur towards the upper range margins of a species (see table S12).

Taken together, this supplementary analysis suggests that the balance of local extinctions and colonizations has shifted over time, with rising extinctions catching up with stable colonizations in the last resurvey. We note that the approach we have used for correcting for lower sampling effort in the resurvey of 2015 (and in a subset of ca. 25% of the plots in 2022) was tailored to correct for overestimating local extinctions and not for underestimating colonizations. However, most (successful) colonizations that may have been overlooked in 2015 should have been counted in 2022, where 75% of the plots were again sampled with the frequency method. As corollary, underestimation of colonizations in 2015 should have been followed by overestimation in the last resurvey in 2022. Nevertheless, in this last resurvey, colonization events were not more frequent than in the first survey in 2008. We hence conclude that the approximately constant number of colonization events across the three resurveys is not a methodological artefact: local extinctions have increased significantly over time but colonizations did not.

Relative elevational ranks of colonizers deviate from the community average in a way exactly opposite to those of the species that went locally extinct: local extinctions are hence more frequent towards the species' lower range margins and colonizations towards the species' upper range margins. These findings strongly suggest climate change as an important driver of the observed dynamics. However, other than in case of local extinctions, exposure to climate warming was not a significant predictor of the number of colonizations. We suppose that this discrepancy is due to stronger context-dependence of colonizations. In particular, due to dispersal limitation in low-statured alpine plants (36,39) the number of newly colonizing species is constrained by the number of potential colonizers in the surrounding of the plots. These pools of potential colonizers will vary considerably in dependence on the richness and composition of regional floras as well as on the surrounding habitat conditions, and this variation is most likely independent of the level of exposure to warming.

All models were fit with the function *glmer()* from the package *lme4 (44)* combined with the package *lmerTest(45)*, marginal and conditional R^2-values were computed with the function *r.squaredGLMM()* from the package *MuMIn* (*46*) in R (*47, version 4.3.2*). Negative binomial models were fit using the function *glmmTMB()* from the package *glmmTMB (48)*. Overdispersion and zero inflation was checked using the function *check_overdispersion()* from the package *performance (49)*.

Table S1.

Number of local extinctions and percentages of all species observations for each time interval and at each of the three levels of spatial aggregation (plot, summit and mountain region). At the plot, summit and mountain region level, local extinctions are counted as species that were not re-observed in a consecutive survey on a plot, the whole summit and the whole mountain region, respectively. Percentages represent averages over all plots, summits or mountain regions per time interval. All values are the mean ± standard deviation of 1000 resamples.

Time interval	***Plot level***	***Summit level***	***Region level***
2001 – 2008	980 ± 0 11.1% ± 0	118 ± 0 6.7% ± 0	57 ± 0 5.5% ± 0
2008 – 2015	1266 ± 9.81 13.7% ± 0.1	154 ± 3.66 8.4% ± 0.2	77 ± 2.50 7.1% ± 0.2
2015 – 2022	1451 ± 8.91 15.7% ± 0.1	185 ± 3.62 9.9% ± 0.2	99 ± 2.40 8.9% ± 0.2

Table S2.

Fixed-effects as well as R^2 values of generalized linear mixed-effects models on proportion data with the number of local extinctions (= species observed in the first, but not in the consecutive survey) and persistences (= species observed in two consecutive surveys) per survey on three different levels of spatial aggregation as the response variable (a two-column variable with the count of successes and failures) and year of survey as the only fixed-effect variable. The model was built assuming a binomial error distribution and a logistic link function. Significant estimates are in bold. The predictor was scaled to zero mean and unit variance. All values are the mean ± standard deviation of 1000 resamples.

	Estimate	***Std. error***	***P value***
Plot level			
R^2m = 0.03 ± 0.001, R^2c = 0.65 ± 0.004			
Proportion local extinctions ~ time + (1|region/summit/plot)			
Intercept	**-1.96 ± 0.005**	0.16 ± 0.002	<0.001 ± 0.000
Time	**0.17 ± 0.003**	0.02 ± 0.000	<0.001 ± 0.000
Summit level			
R^2m = 0.09 ± 0.008*, R^2c* = 0.73 ± 0.011			
Proportion local extinctions ~ time + (1|region/summit)			
Intercept	**-2.46 ± 0.010**	0.13 ± 0.003	<0.001 ± 0.000
Time	**0.19 ± 0.010**	0.05 ± 0.000	<0.001 ± 0.000
Mountain region level			
R^2m = 0.17 ± 0.018*, R^2c* = 0.81 ± 0.010			
Proportion local extinctions ~ time + (1|region)			
Intercept	**-2.65 ± 0.015**	0.11 ± 0.004	<0.001 ± 0.000
Time	**0.21 ± 0.013**	0.04 ± 0.000	<0.001 ± 0.000

Table S3.

Fixed-effects as well as R^2values of generalized linear mixed-effects models on count data with the number of species per survey on three different levels of spatial aggregation as the response variable and year of survey as the only fixed- effect predictor variable. The model was built assuming a Poisson error distribution and a logistic link function and was checked for overdispersion using the function *check_overdispersion()* from the package *performance*. Significant estimates are in bold. The predictor was scaled to zero mean and unit variance. All values are the mean ± standard deviation of 1000 resamples.

	Estimate	***Std. error***	***P value***
Plot level			
R^2m = 0.0002 ± 0.0000*, R^2c = 0.9102* ± 0.0003			
Species richness ~ time + (1|region/summit/plot)			
Intercept	**1.89 ± 0.001**	0.15 ± 0.000	<0.001 ± 0.000
Time	**0.01 ± 0.000**	0.01 ± 0.000	0.008 ± 0.001
Summit level			
R^2m = 0.0006 ± 0.000*, R^2c* = 0.9630 ± 0.0002			
Species richness ~ time + (1|region/summit)			
Intercept	**3.06 ± 0.001**	0.16 ± 0.000	<0.001 ± 0.000
Time	**0.02 ± 0.000**	0.01 ± 0.000	0.049 ± 0.004
Mountain region level			
R^2m = 0.0010 ± 0.000*, R^2c* = 0.9671 ± 0.0002			
Species richness ~ time + (1|region)			
Intercept	**4.05 ± 0.001**	0.16 ± 0.000	<0.001 ± 0.000
Time	0.02 ± 0.000	0.02 ± 0.000	0.168 ± 0.008

Table S4.

Fixed-effects as well as R^2-values of a linear mixed-effects model on total vegetation cover per plot per survey as the response variable and year of survey as the only fixed-effect variable. Significant estimates are in bold. The predictor was scaled to zero mean and unit variance. All values are the mean ± standard deviation of 1000 resamples.

	Estimate	***Std. error***	***P value***
Plot level			
R^2m = 0.002 ± 0.0000, *R^2c = 0.9204* ± 0.0000			
Plot cover ~ time + (1|region/summit/plot)			
Intercept	**40.34± 0.000**	6.57 ± 0.000	<0.001 ± 0.000
Time	**1.49 ± 0.000**	0.18 ± 0.000	<0.001 ± 0.000

Table S5.

Fixed-effects as well as R^2 values of generalized linear mixed-effects models on proportion data with the number of local extinctions (= species observed in the first, but not in the consecutive survey) and persistences (= species observed in two consecutive surveys) per survey on three different levels of spatial aggregation as the response variable (a two-column variable with the count of successes and failures) and climate warming as the only fixed-effect variable. The model was built assuming a binomial error distribution and a logistic link function. Significant estimates are in bold. The predictor was scaled to zero mean and unit variance. All values are the mean ± standard deviation of 1000 resamples.

	Estimate	***Std. error***	***P value***
Plot level			
R^2m = 0.14 ± 0.004, R^2c = 0.68 ± 0.004			
Proportion local extinctions ~ climate warming + (1|region/summit/plot)			
Intercept	**-1.98 ± 0.005**	0.16 ± 0.002	<0.001 ± 0.000
Climate warming	**0.38 ± 0.005**	0.03 ± 0.000	<0.001 ± 0.000
Summit level			
R^2m = 0.27 ± 0.014, *R^2c* = 0.78 ± 0.009			
Proportion local extinctions ~ climate warming + (1|region/summit)			
Intercept	**-2.49 ± 0.001**	0.13 ± 0.003	<0.001 ± 0.000
Climate warming	**0.37 ± 0.015**	0.08 ± 0.001	<0.001 ± 0.000
Mountain region level			
R^2m = 0.36 ± 0.018, *R^2c* = 0.89 ± 0.008			
Proportion local extinctions ~ climate warming + (1|region)			
Intercept	**-2.68 ± 0.015**	0.13 ± 0.004	<0.001 ± 0.000
Climate warming	**0.39 ± 0.020**	0.06 ± 0.000	<0.001 ± 0.000

Table S6.

Fixed-effects as well as R^2 values of generalized linear mixed-effects models on proportion data with the number of local extinctions (= species observed in the first, but not in the consecutive survey) and persistences (= species observed in two consecutive surveys) per survey on three different levels of spatial aggregation as the response variable (a two-column variable with the count of successes and failures) and climate warming, latitude and longitude as fixed-effect variables. The model was built assuming a binomial error distribution and a logistic link function. Significant estimates are in bold. All predictors were scaled to zero mean and unit variance. All values are the mean ± standard deviation of 1000 resamples.

	Estimate	***Std. error***	***P value***
Plot level *R^2m* = 0.35 ± 0.007, *R^2c* = 0.67 ± 0.004 *Proportion local extinctions ~ climate warming + Latitude + Longitude + (1|region/summit/plot)*			
Intercept	**-1.99 ± 0.005**	0.10 ± 0.002	<0.001 ± 0.000
Climate warming	**0.38 ± 0.005**	0.03 ± 0.000	<0.001 ± 0.000
Latitude	**-0.42 ± 0.009**	0.11 ± 0.002	<0.001 ± 0.000
Longitude	0.15 ± 0.005	0.10 ± 0.002	0.16 ± 0.016
Summit level *R^2m* = 0.33 ± 0.021, *R^2c* = 0.78 ± 0.009 *Proportion local extinctions ~ climate warming + Latitude + Longitude + (1|region/summit)*			
Intercept	**-2.52 ± 0.011**	0.12 ± 0.003	<0.001 ± 0.000
Climate warming	**0.38 ± 0.015**	0.08 ± 0.001	<0.001 ± 0.000
Latitude	-0.17 ± 0.021	0.14 ± 0.003	0.21 ± 0.055
Longitude	0.05 ± 0.009	0.12 ± 0.004	0.65 ± 0.052
Mountain region level *R^2m* = 0.35 ± 0.022, *R^2c* = 0.88 ± 0.008 *Proportion local extinctions ~ climate warming + Latitude + Longitude + (1|region)*			
Intercept	**-2.69 ± 0.016**	0.13 ± 0.005	<0.001 ± 0.000
Climate warming	**0.40 ± 0.021**	0.06 ± 0.000	<0.001 ± 0.000
Latitude	-0.07 ± 0.023	0.13 ± 0.005	0.61 ± 0.127
Longitude	0.12 ± 0.015	0.12 ± 0.005	0.33 ± 0.061

Table S7.

Fixed effects as well as R^2-values of logistic generalized linear mixed-effects models with local extinction (binary, yes/no) as response. The predictors were the average cover change between 2 surveys, approximately 7 or 14 years, the cover at the beginning of the respective time interval; and for the last model additionally the relative elevational rank of each species in a plot. All predictors were scaled to zero mean and unit variance. All values are the mean ± standard deviation of 1000 resamples.

	Estimate	***Std. error***	***P value***
Time period: 7 years R^2m = 0.58 ± 0.004, R^2c = 0.73 ± 0.003 *Local extinctions ~ cover 2008 + average cover change + (1|region/summit) + (1|Species)*			
Intercept	**-3.43± 0.013**	0.25 ± 0.002	<0.001 ± 0.000
Av. cover change 7 years	**-1.24 ± 0.015**	0.17 ± 0.001	<0.001 ± 0.000
Cover 2008	**-2.72 ± 0.022**	0.28 ± 0.001	<0.001 ± 0.000
Time period: 14 years R^2m = 0.60 ± 0.004, R^2c = 0.74 ± 0.003 *Local extinctions ~ cover 2001 + average cover change + (1|region/summit) + (1|Species)*			
Intercept	**-3.46 ± 0.014**	0.25 ± 0.002	<0.001 ± 0.000
Av. cover change 14 years	**-1.50 ± 0.018**	0.18 ± 0.001	<0.001 ± 0.000
Cover 2001	**-2.77 ± 0.024**	0.28 ± 0.001	<0.001 ± 0.000
Time period: 14 years R^2m = 0.75 ± 0.042, R^2c = 0.83 ± 0.028 *Local extinctions ~ cover 2001 + average cover change + relative elevational rank + thermophilization+ (1|region/summit) + (1|Species)*			
Intercept	**-3.89 ± 0.202**	0.26 ± 0.010	<0.001 ± 0.000
Av. cover change 14 years	**-2.06 ± 0.287**	0.24 ± 0.024	<0.001 ± 0.000
Cover 2001	**-3.90 ± 0.531**	0.37 ± 0.038	<0.001 ± 0.000
Relative elevational rank	**0.16 ± 0.008**	0.06 ± 0.002	0.01 ± 0.005
Thermophilization	**0.18 ± 0.015**	0.09 ± 0.006	0.04 ± 0.006

Table S8.

Description of all 62 summits including the number of plots per summit and the year of the 4 surveys. On one summit (Zinken-NW-summit, AT) the plots were surveyed in two different years in survey 1.

Mountain region	Country	Summit	Elevation	Latitude	Longitude	Number of plots	Year of Survey1	Year of Survey 2	Year of Survey 3	Year of Survey 4
Dovrefjell (S-Scandes)	NO	Vesle Armodshokollen	1161	62.2621	9.66582	16	2001	2008	2015	2022
Dovrefjell (S-Scandes)	NO	Veslekolla	1418	62.30665	9.4573	16	2001	2008	2015	2022
Dovrefjell (S-Scandes)	NO	Kolla	1651	62.29214	9.48661	8	2001	2008	2015	2022
Dovrefjell (S-Scandes)	NO	Storkinn	1845	62.34667	9.44069	3	2001	2008	2015	2022
Cairngorms (Scotland)	UK	Creag Mhigeachaidh	742	57.09862	-3.86096	16	2002	2008	2015	2022
Cairngorms (Scotland)	UK	Camp Cairn	904	57.09029	-3.84285	15	2001	2008	2015	2022
Cairngorms (Scotland)	UK	Unknown Hillock	978	57.07944	-3.83	16	2001	2008	2015	2022
Cairngorms (Scotland)	UK	Sgoran Dubh Mor	1111	57.07972	-3.80944	16	2001	2008	2015	2022
W-Carpathians / High Tatra	SK	Krížna	1919	49.18083	19.94972	16	2002	2008	2015	2022
W-Carpathians / High Tatra	SK	Velká kopa	2052	49.20056	19.97361	16	2002	2008	2015	2022
W-Carpathians / High Tatra	SK	Sedielková kopa	2061	49.14972	20.02056	16	2001	2008	2015	2022
W-Carpathians / High Tatra	SK	Krátka	2336	49.16306	20.01444	16	2002	2008	2015	2022
NE-Alps / Hochschwab	AT	Zinken-NW-summit	1910	47.59826	15.09152	16	1998/2002	2008	2015	2022
NE-Alps / Hochschwab	AT	Weihbrunnkogel	2065	47.62474	15.16285	16	2001	2008	2015	2022
NE-Alps / Hochschwab	AT	G´hacktkogel	2214	47.61389	15.13152	16	2001	2008	2015	2022
NE-Alps / Hochschwab	AT	Zagelkogel-NW-summit	2255	47.61076	15.12332	16	2001	2008	2015	2022
E-Carpathians / Rodnei Mts.	RO	Gropile	2063	47.57253	24.61761	16	2001	2008	2015	2022
E-Carpathians / Rodnei Mts.	RO	Golgota	2116	47.60049	24.62521	16	2001	2008	2015	2022
E-Carpathians / Rodnei Mts.	RO	Buhaiescu	2221	47.58266	24.63246	16	2001	2008	2015	2022
E-Carpathians / Rodnei Mts.	RO	Rebra	2268	47.58563	24.63577	16	2001	2008	2015	2022
Central Alps / Swiss National Park - siliceous	CH	Mot sper Chamana Sesvenna	2424	46.73565	10.4286	16	2003	2010	2015	2022

Central Alps / Swiss National Park - siliceous	CH	Minschuns	2519	46.64543	10.33792	16	2002	2010	2015	2022
Central Alps / Swiss National Park - siliceous	CH	Mot dal Gajer	2797	46.69434	10.3311	16	2002	2010	2015	2022
Central Alps / Swiss National Park - siliceous	CH	Piz Plazer	3104	46.70862	10.388	7	2002	2010	2015	2022
Central Alps / Swiss National Park - carbonatic	CH	Munt Buffalora	2438	46.63856	10.24364	16	2003	2009	2015	2022
Central Alps / Swiss National Park - carbonatic	CH	Munt Chavagl	2542	46.64419	10.23407	12	2002	2009	2015	2022
Central Alps / Swiss National Park - carbonatic	CH	Piz Murtèr	2836	46.64578	10.14171	14	2002	2009	2015	2022
Central Alps / Swiss National Park - carbonatic	CH	Piz Foraz	3092	46.69075	10.27672	11	2002	2009	2015	2022
S-Alps / Dolomites	IT	Grasmugl	2199	46.33082	11.56248	16	2001	2008	2015	2022
S-Alps / Dolomites	IT	Do Peniola	2463	46.38282	11.60545	14	2001	2008	2015	2022
S-Alps / Dolomites	IT	Ragnaroek	2757	46.38368	11.59267	15	2001	2008	2015	2022
S-Alps / Dolomites	IT	Monte Schutto	2893	46.5247	11.81478	15	2001	2008	2015	2022
W-Alps / Alps of Valais-Entremont	CH	La Ly	2360	46.03076	7.24917	16	2001	2008	2015	2022
W-Alps / Alps of Valais-Entremont	CH	Mont Brûlé	2550	46.02057	7.20137	16	2001	2008	2015	2022
W-Alps / Alps of Valais-Entremont	CH	Pointe du Parc	2989	45.99798	7.23227	7	2001	2008	2015	2022
W-Alps / Alps of Valais-Entremont	CH	Pointe de Boveire	3212	45.99452	7.24003	4	2001	2008	2015	2022
W-Alps / Mont Avic	IT	Colle Lago Bianco	2340	45.64639	7.59499	16	2002	2012	2017	2022
W-Alps / Mont Avic	IT	Lago Balena	2584	45.64026	7.5516	16	2002	2012	2017	2022
W-Alps / Mont Avic	IT	Pra Pelat	2790	45.65891	7.54782	15	2002	2012	2017	2022
W-Alps / Mont Avic	IT	Cime Bianche	3014	45.91941	7.69407	16	2002	2012	2017	2022
Northern Apennines	IT	Cima di Foce a Giovo	1722	44.11833	10.61083	16	2001	2008	2015	2022

Northern Apennines	IT	Cima di Pian Cavallaro	1815	44.2025	10.6925	16	2001	2008	2015	2022
Northern Apennines	IT	Alpe di Mommio	1854	44.27583	10.24472	16	2001	2008	2015	2022
Northern Apennines	IT	Monte Casarola	1978	44.33167	10.2075	12	2001	2008	2015	2022
Central Pyrenees / Ordesa	ES	Punta Acuta	2242	42.63758	-0.06232	16	2001	2008	2015	2022
Central Pyrenees / Ordesa	ES	Sierra Custodia	2519	42.65004	0.03266	16	2001	2008	2015	2022
Central Pyrenees / Ordesa	ES	Punta Tobacor	2779	42.65514	-0.01309	12	2001	2008	2015	2022
Central Pyrenees / Ordesa	ES	Punta de las Olas	3022	42.66227	0.05394	7	2001	2008	2015	2022
Central Caucasus / Kazbegi region	GE	Cross Pass 1	2240	42.53944	44.49306	16	2001	2008	2015	2022
Central Caucasus / Kazbegi region	GE	Cross Pass 2	2477	42.49917	44.45639	16	2001	2008	2015	2022
Central Caucasus / Kazbegi region	GE	Cross Pass 4 - Kudebi	3024	42.49694	44.51	16	2001	2008	2015	2022
Central Apennines / Majella	IT	Femmina Morta	2405	42.03321	14.09924	16	2001	2008	2015	2022
Central Apennines / Majella	IT	Monte Macellaro	2635	42.05804	14.10121	16	2001	2008	2015	2022
Central Apennines / Majella	IT	Monte Mammoccio	2737	42.10354	14.12095	16	2001	2008	2015	2022
Sierra Nevada - West	ES	Pulpitito	2778	37.03667	-3.34528	16	2001	2008	2015	2022
Sierra Nevada - West	ES	Cúpula	2968	37.04583	-3.35222	16	2001	2008	2015	2022
Sierra Nevada - West	ES	Pico del Tosal Cartujo	3150	37.03972	-3.405	16	2001	2008	2015	2022
Sierra Nevada - West	ES	Cerro de los Machos	3327	37.05722	-3.3575	11	2001	2008	2015	2022
Crete / Lefka Ori	GR	low summit	1664	35.26861	24.08722	16	2001	2008	2015	2022
Crete / Lefka Ori	GR	Chorafas	1965	35.27333	24.08111	16	2001	2008	2015	2022
Crete / Lefka Ori	GR	South-East of Kakovoli	2160	35.28444	24.09083	16	2001	2008	2015	2022
Crete / Lefka Ori	GR	Sternes	2339	35.29667	24.05667	10	2001	2008	2015	2022

886

Table S9.

Number of local colonizations for each time interval and at each of the three levels of spatial aggregation (plot, summit and mountain region). At the plot, summit and mountain region level, local colonizations were counted as species that were observed in one resurvey, but were not observed in the previous one. All values are the mean ± standard deviation of 1000 resamples.

Time interval	***Plot level***	***Summit level***	***Region level***
2001 – 2008	1391 ± 0	194 ± 0	102 ± 0
2008 – 2015	1284 ± 0	189 ± 0	99 ± 0
2015 – 2022	1401 ± 5.57	191 ± 1.83	95 ± 1.45

Table S10.

Fixed-effects as well as R^2 values of generalized linear mixed-effects models on count data with the number of local colonizations per survey on three different levels of spatial aggregation as the response variable and year of survey as the only fixed-effect variable. The model was built assuming a negative binomial error distribution and a logistic link function. Significant estimates are in bold. The predictor was scaled to zero mean and unit variance. All values are the mean ± standard deviation of 1000 resamples.

	Estimate	***Std. error***	***P value***
Plot level			
R^2m = 0.00 ± 0.000, R^2c = 0.25 ± 0.003			
Number local colonizations~ time + (1|region/summit/plot)			
Intercept	**0.37 ± 0.003**	0.10 ± 0.001	<0.001 ± 0.000
Time	0.02 ± 0.002	0.02 ± 0.000	0.17 ± 0.033
Summit level			
R^2m = 0.00 ± 0.000, *R^2c* = 0.34 ± 0.007			
Number local colonizations ~ time + (1|region/summit)			
Intercept	**1.06 ± 0.008**	0.12 ± 0.002	<0.001 ± 0.000
Time	-0.00 ± 0.006	0.05 ± 0.000	0.92 ± 0.053
Mountain region level			
R^2m = 0.17 ± 0.018, *R^2c* = 0.81 ± 0.010			
Number local colonizations ~ time + (1|region)			
Intercept	**1.65 ± 0.015**	0.16 ± 0.007	<0.001 ± 0.000
Time	**-0.03 ± 0.007**	0.03 ± 0.000	0.31 ± 0.101

Table S11.

Fixed-effects as well as R^2 values of generalized linear mixed-effects models on count data with the number of local colonizations per survey on three different levels of spatial aggregation as the response variable and climate warming as the only fixed-effect variable. The model was built assuming a negative binomial error distribution and a logistic link function. Significant estimates are in bold. The predictor was scaled to zero mean and unit variance. All values are the mean ± standard deviation of 1000 resamples.

	Estimate	***Std. error***	***P value***
Plot level			
R^2m = 0.00 ± 0.000, R^2c = 0.25 ± 0.003			
Number local colonizations ~ climate warming + (1|region/summit/plot)			
Intercept	**0.37 ± 0.003**	0.10 ± 0.001	<0.001 ± 0.000
Climate warming	0.02 ± 0.003	0.03 ± 0.000	0.51 ± 0.068
Summit level			
R^2m = 0.00 ± 0.001, *R^2c* = 0.33 ± 0.008			
Number local colonizations ~ climate warming + (1|region/summit)			
Intercept	**1.06 ± 0.008**	0.12 ± 0.002	<0.001 ± 0.000
Climate warming	0.04 ± 0.007	0.08 ± 0.001	0.61 ± 0.060
Mountain region level			
R^2m = 0.01 ± 0.003, *R^2c* = 0.72 ± 0.025			
Number local colonizations ~ climate warming + (1|region)			
Intercept	**1.65 ± 0.016**	0.17 ± 0.008	<0.001 ± 0.000
Climate warming	-0.07 ± 0.013	0.06 ± 0.000	0.21 ± 0.084

Table S12.

Intercept as well as R^2 values of intercept-only linear mixed-effects models with the relative elevational rank of colonizers per resurvey on three different levels of spatial aggregation as the response. Significant estimates are in bold. All values are the mean ± standard deviation of 1000 resamples.

	Estimate	***Std. error***	***P value***
Plot level *R^2c = 0.06 ± 0.002* *Relative elevational rank~ 1 + (1|region/summit/plot)*			
Intercept	**-0.23 ± 0.003**	0.05 ± 0.001	<0.001 ± 0.000
Summit level *R^2c* = 0.01 ± 0.004 *Relative elevational rank~ 1 + (1|region/summit)*			
Intercept	**-0.53 ± 0.006**	0.06 ± 0.002	<0.001 ± 0.000
Mountain region level *R^2c* = 0.08 ± 0.011 *Relative elevational rank~ 1 + (1|region)*			
Intercept	**- 0.65 ± 0.010**	0.11 ± 0.004	<0.001 ± 0.000

917